Oscillatory thermomagnetic instability in superconducting films

J. I. Vestgården,[1,2] Y. M. Galperin,[1,3] and T. H. Johansen[1,4]

[1] *Department of Physics, University of Oslo, P. O. Box 1048 Blindern, 0316 Oslo, Norway*
[2] *Norwegian Defence Research Establishment (FFI), Kjeller, Norway*
[3] *Ioffe Physical Technical Institute, 26 Polytekhnicheskaya, St Petersburg 194021, Russian Federation*
[4] *Institute for Superconducting and Electronic Materials, University of Wollongong, Innovation Campus, Squires Way, North Wollongong NSW 2500, Australia*

The stability of superconducting films with respect to an oscillatory thermomagnetic instability is investigated. Closed expressions for the threshold magnetic field and temperature are derived based on linear stability analysis. We find that the oscillatory modes turn unstable at much lower electric field than other modes and they are hence also the most dangerous with respect to nucleation of dendritic flux avalanches.

PACS numbers: 74.25.Ha, 68.60.Dv, 74.78.-w

I. INTRODUCTION

The irreversible electromagnetic properties of type-II superconductors are commonly explained in terms of the critical current density j_c, as introduced by Bean.[1] In the corresponding critical state the distribution of magnetic flux is nonuniform and metastable. However, since j_c is a decreasing function of temperature the metastable state can suffer from an instability driven by the Joule heat generated during flux motion. In bulk superconductors this thermomagnetic instability gives rise to abrupt entry of large amounts of flux, so-called flux jumps, which may cause the entire superconductor to be heated to the normal state.[2–6] In some cases, pronounced oscillations in the magnetization and temperature have been detected prior to such flux jumps.[7,8]

In film superconductors experiencing transverse magnetic fields, the same instability gives rise to abrupt flux penetration in the form of dendritic structures rooted at the sample edge.[9] Using magneto-optical imaging (MOI) the residual flux distribution left in the film after such avalanche events[10] have been observed in many superconducting materials.[11–15] The experiments also show that there is a threshold magnetic field, $H_{\rm th}$, for the onset of avalanche activity, and that the unstable behavior is restricted to temperatures below a threshold value, $T_{\rm th}$, see Fig. 1. These thresholds have been explained on the basis of linear stability analysis of the nonlinear and nonlocal equations governing the electrodynamics of such films.[16–23] Moreover, those theoretical works show that in order to trigger an avalanche electrical fields in the range $E = 30$-100 mV/m are required.

Experimentally, one finds in films of many superconductors, such as MgB_2, Nb and NbN, that avalanches occur even when the magnetic field is ramped very slowly, thus inducing correspondingly small electric fields. For films some millimeters in lateral size, $2w$, placed in a magnetic field ramped at a rate of $\mu_0\dot{H}_a = 10$ mT/s, the electric field along the edge can be estimated[24] to $\mu_0\dot{H}_a w \sim 10\ \mu$V/m, i.e., far below the theoretical threshold values. This inconsistency led to the suggestion[25] that micro-avalanches of non-thermomagnetic origin are initial precursors, which in turn trigger the large and powerful thermomagnetic avalanches in superconducting films.

In the present work the vast discrepancy in the onset electrical fields is addressed theoretically. By analysing modes with a complex instability increment, i.e., considering scenarios involving oscillatory precursor behavior, it is found that superconducting films become unstable at much smaller electric fields than previously expected. This shows that the instability can develop directly from the low E-field background of the critical state, without involving micro-avalanches of unknown origin. The presented theory is fully quantitative and depends only on measurable parameters. Several aspects of the analytical results are verified by quantitative comparison with numerical solutions of the full nonlinear thermomagnetic problem.

II. MODEL

Consider a superconducting film shaped as a strip of thickness d and width $2w$, where $w \gg d$. The strip is very long in the y-direction, and has thermal contact with a substrate, see Fig. 2. The sample is initially zero-field cooled to a temperature, T, below the superconducting transition temperature, T_c, whereupon a perpendicular magnetic field H_a is applied at a constant rate $\dot{H}_a$.

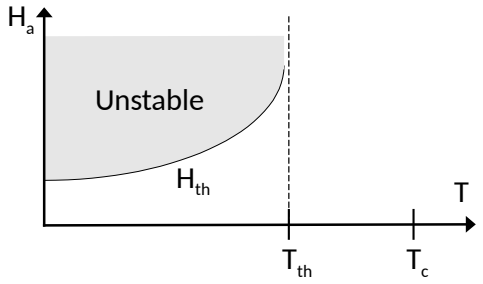

FIG. 1. Generic thermomagnetic stability diagram of film superconductors.

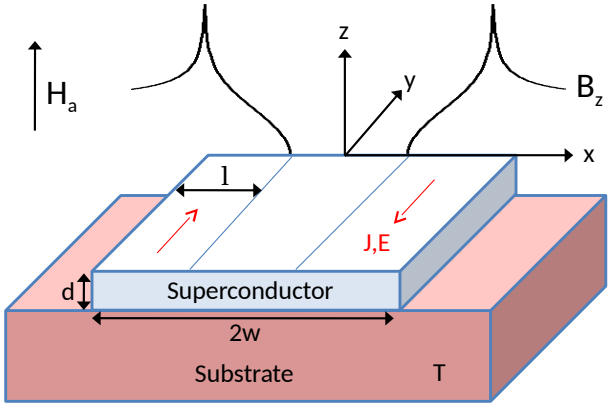

FIG. 2. (Color online) Sample geometry: A long superconducting strip in thermal contact with a substrate experiencing an increasing magnetic field H_a applied along the z-axis, inducing currents and electrical fields in the y-direction.

Assuming that the overall flux dynamics in the superconductor follows the Bean model, the flux will penetrate to a depth l increasing with the applied field as[26]

$$l/w = 1 - \cosh^{-1}(\pi H_a/dj_c). \tag{1}$$

This flux motion induces an electrical field, which is maximum at the strip edge where the value is given by,[24]

$$E_{\rm edge} = \mu_0 \dot{H}_a w \tanh\left(\pi H_a/dj_c\right). \tag{2}$$

For perturbations of the Bean state, we describe the superconductor using the more general model,[27]

$$\mathbf{E} = \begin{cases} \rho_n \left(J/dj_c\right)^{n-1} \mathbf{J}/d, & J < dj_c \text{ and below } T_c, \\ \rho_n \mathbf{J}/d, & \text{otherwise.} \end{cases} \tag{3}$$

Here, $\mathbf{J}$ is the sheet current, ρ_n is the normal state resistivity, and n is the flux creep exponent. The Bean model corresponds to the limit $n \to \infty$.

The electrodynamics follows the Maxwell equations

$$\dot{\mathbf{B}} = -\nabla \times \mathbf{E}, \quad \nabla \times \mathbf{H} = \mathbf{J}\delta(z), \quad \nabla \cdot \mathbf{B} = 0, \tag{4}$$

with $\nabla \cdot \mathbf{J} = 0$, $\mu_0 \mathbf{H} = \mathbf{B}$. The heat-flow in the strip is described by

$$c\dot{\tilde{T}} = \kappa \nabla^2 \tilde{T} - \frac{h}{d}(\tilde{T} - T) + \frac{1}{d}\mathbf{J} \cdot \mathbf{E}, \tag{5}$$

where $\tilde{T}$ is the local temperature in the superconductor, and T is the uniform substrate temperature. The superconductor's specific heat is c, its thermal conductivity is κ, and h is the coefficient of heat transfer between the strip and the substrate. The temperature dependencies are chosen as $c = c_0(\tilde{T}/T_c)^3$, $\kappa = \kappa_0(\tilde{T}/T_c)^3$, and $h = h_0(\tilde{T}/T_c)^3$. For the electrodynamical parameters we use $j_c = j_{c0}(1 - \tilde{T}/T_c)$ and $n = n_0 T_c/\tilde{T}$.

III. THRESHOLDS AND OSCILLATION FREQENCIES

To find the characteristics of the behavior near the onset of an avalanche consider first the threshold electric field, $E_{\rm th}$. In Ref. 28 it was shown based on the Eqs. (3)–(5), that at low T the threshold condition can be expressed as

$$\frac{j_c}{T^*} n E_{\rm th} - \kappa k^2 - \frac{h}{d} - \frac{2}{k}\left(k_x^2 + \frac{k_y^2}{n}\right)\frac{c}{\mu_0 d j_c} n E_{\rm th} = 0. \tag{6}$$

Here, $T^* = 1/|\partial \ln j_c/\partial T|$ and k_x and k_y are the Fourier space wave-vectors. It was also found that the instability is accompanied by temporal oscillations with a frequency, ω, given by

$$\omega^2 = \frac{2}{k}\frac{n E_{\rm th}}{\mu_0 d j_c c} \times \left[\left(k_x^2 + \frac{k_y^2}{n}\right)\left(\kappa k^2 + \frac{h}{d}\right) + \left(k_x^2 - k_y^2\right)\frac{j_c E_{\rm th}}{T^*}\right]. \tag{7}$$

As H_a increases from zero, the most unstable modes are,[28] $k_y = 0$ and $k_x = \pi/2l$, and in what follows only these modes are considered.

First, at small H_a, the main mechanism for suppression of the instability is the lateral heat diffusion. Thus, neglecting in Eq. (6) the terms proportional to c and h, one obtains

$$E_{{\rm th},\kappa} = \frac{\kappa T^*}{n j_c}\left(\frac{\pi}{2l}\right)^2. \tag{8}$$

For small H_a, the Eq. (1) gives $l \approx (w/2)(\pi H_a/dj_c)^2$, and from Eq. (2) the electric field is $E_{\rm edge} \approx \mu_0 \dot{H}_a w \pi H_a/dj_c$. Inserting these limiting expressions in Eq. (8) the threshold applied magnetic field becomes,

$$H_{{\rm th},\kappa} = \frac{dj_c}{\pi}\left(\frac{\pi^2 \kappa T^*}{n w^3 j_c \mu_0 \dot{H}_a}\right)^{1/5}. \tag{9}$$

This formula gives the threshold field as a function of T through the temperature dependencies of κ, j_c and n. The corresponding oscillation frequency, calculated from Eq. (7) assuming $n \gg 1$, is

$$\omega_\kappa = \mu_0 \dot{H}_a n \sqrt{\frac{2\pi w}{\mu_0 d c T^*}}, \tag{10}$$

which depends on temperature through n, c and T^*.

Then, at deeper penetration, when $l \gg (\pi/2)\sqrt{\kappa d/h}$, the main mechanism suppressing the instability is heat removal by the substrate. In this case one can in Eq. (6) ignore the terms propotional to κ and c, which gives

$$E_{{\rm th},h} = \frac{hT^*}{n d j_c}. \tag{11}$$

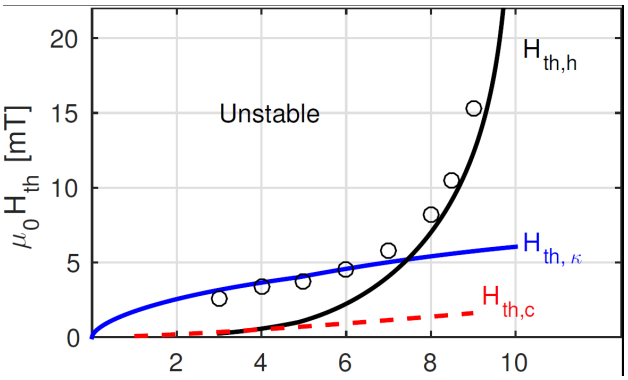

FIG. 3. (Color online) Threshold magnetic fields $H_{\mathrm{th},\kappa}$ (blue), $H_{\mathrm{th},h}$ (black), and $H_{\mathrm{th,c}}$ (dashed red), as functions of temperature. The discrete data represent the numerical results. The simulations used parameters for MgB_2, see the main text.

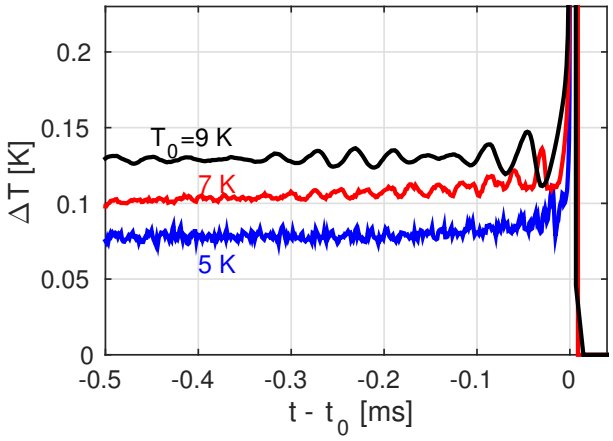

FIG. 4. (Color online) Temporal variations in temperature prior to typical avalanches at 3 different substrate temperatures.

Combining this with Eq. (2) to eliminate the E-field one obtains the following threshold magnetic field,[29]

$$H_{\mathrm{th},h} = \frac{dj_c}{\pi}\,\mathrm{atanh}\left(\frac{hT^*}{ndj_c\mu_0\dot{H}_a w}\right). \qquad (12)$$

Also this case is accompanied by oscillations, and at full penetration, when $E \approx \mu_0\dot{H}_a w$, the frequency is

$$\omega_h = \omega_\kappa/\sqrt{2}\,. \qquad (13)$$

The actual oscillation frequency is, for most temperatures, between ω_h and ω_κ.

From Eq. (12) it follows that $H_{\mathrm{th},h}$ diverges when

$$\frac{hT^*}{ndj_c\mu_0\dot{H}_a w} = 1.$$

Thus, when the left hand side exceeds unity a thermomagnetic instability is not possible, and is therefore the condition that determines the threshold temperature, T_{th}. From this one finds

$$T_{\mathrm{th}}/T_c = (\mu_0\dot{H}_a j_{c0} n_0 w d/T_c h_0)^{1/4}, \qquad (14)$$

using the temperature dependences of j_c, n and h given above.

Finally, consider the adiabatic condition, i.e., when the instability is prevented only by the heat capacity of the superconductor. The threshold follows then from Eq. (6) with $\kappa = h = 0$. Using k_x with $l(H_a)$ in its shallow penetration form, the result becomes

$$H_{\mathrm{th,c}} = \sqrt{\frac{2}{\pi}\frac{cT^*}{\mu_0}\frac{d}{w}}\,. \qquad (15)$$

This expression was reported also previously[18,19]. Note that the adiabatic threshold magnetic field is independent of the field ramp rate, unlike both $H_{\mathrm{th},\kappa}$ and $H_{\mathrm{th},h}$. (BUT no oscillations ?)

IV. NUMERICAL SIMULATIONS

To verify these theoretical predictions near onset of the thermomagnetic instability, the set of full equations (3) - (5) were solved numerically.[22] This was carried out using material parameters typical for films of MgB_2,[20,30?] i.e., $c_0 = 35\cdot 10^3$ J/m, $\kappa_0 = 160$ W/Km^3, $\rho_n = 7\cdot 10^{-8}$ Ωm, $j_{c0} = 1\cdot 10^{11}$ Am^{-2}, $n_0 = 50$, and $T_c = 39$ K. The ramp rate was set to $\mu_0\dot{H}_a = 600$ mT/s, and the sample dimensions, $w = 2$ mm and $d = 0.5$ μm, were used. The creep exponent was limited to $n = 400$ at low temperatures. The substrate cooling parameter, not known from measurements, was taken as $h_0 = 1.8\cdot 10^4$ W/Km^2 to give $T_{\mathrm{th}} = 10$ K in accordance with Eq. (14) and experimental observations.[31] Numerical results were obtained for temperatures $T = 3, 4, \ldots, 10$ K.

Shown in Fig. 3 is the threshold magnetic field plotted as function of temperature. The full curves represent the analytical expressions $H_{\mathrm{th},\kappa}$, $H_{\mathrm{th},h}$ and $H_{\mathrm{th,c}}$, while the discrete data show the simulation results. Each data point indicates the applied field when the first avalanche occurs as the field increases from zero. For $T = 10$ K the simulations gave no avalanche activity.

From the figure one sees that for $T < 7$ K, the graph representing $H_{\mathrm{th},\kappa}$ gives an excellent fit to the numerical data. Above 7 K the data cross over to follow closely the curve representing $H_{\mathrm{th},h}$. Note that the curve for the adiabatic threshold lies far below the numerical data, and thus, does not represent a relevant mechanism at any temperature for the present material parameters and field ramp rate.

Direct evidence for oscillatory behavior preceeding the onset of avalanches is presented in Fig. 4. The figure shows temporal fluctuations in the temperature over an interval of 0.5 ms prior to avalanche events taking place at 3 different temperatures. The t_0 is the time of avalanche onset. The graph obtained at 9 K shows in the whole time interval clear oscillations with one dominant fre-

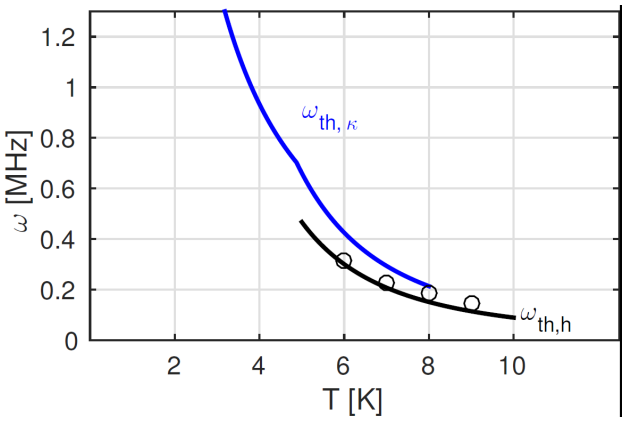

FIG. 5. (Color online) Oscillation frequencies as functions of temperature. The discrete data represent the numerical results.

quency. During the last 0.1 ms before $t = t_0$ the amplitude is growing significantly. A quite similar behavior is evident also in the graph obtained at $T = 7$ K. The oscillations are here smaller in amplitude, and noise is more pronounced. Neverthess, nearly harmonic oscillations are seen during the last 0.3 ms before onset, and their frequency is larger than at 9 K. Like at 9 K the oscillation amplitude increases towards the onset. In addition, the dc-part of the ΔT signal also increases slightly towards time t_0. At 5 K, on the other hand, the noise dominates the behavior, and a characteristic frequency was not found. The dc-part of ΔT increases also here when approaching the onset.

The characteristic frequency, ω, obtained numerically for temperatures between 6 K and 9 K are shown as descrete data in Fig. 5. The ω was obtained from the location of the peak in the Fourier spectrum of the excess temperature, ΔT prior to avalanches. The full curves in the figure show the analytical expressions ω_κ and ω_h. Evidently, the decrease in ω with increasing temperature is following the curve for $\omega_h(T)$ extremely well.

V. DISCUSSION

Let us first compare the results with previous analytical works. According to Ref. 20, the electric field threshold for non-oscillatory modes is

$$E_{\rm th} = \frac{T^*}{j_c}\left(\frac{\pi}{2l}\sqrt{\kappa} + \sqrt{\frac{h}{nd}}\right)^2 . \qquad (16)$$

In the low T limit, where we can put $h = 0$, we see that Eq. (16) is a factor n higher than the oscillatory threshold in Eq. (8). Because n is very large in many materials, this implies that the oscillatory instability are significantly more dangerous than the non-oscillatory instability. In the other limit, when $h = 0$, Eqs. (16) and (11) coincide.

Let us then discuss the consequences of the results of this work and its implications for experiments. First we notice that in hard superconductor, with $n \to \infty$, the threshold is actually set by the adiabatic condition, $H_{{\rm th},c}$. The same is also true in the limits $\dot{H}_a \to \infty$, $d \to 0$, and $j_c \to 0$. Second, for superconductors with finite n and at sufficiently low $\dot{H}_a$, the threshold at shallow penetration is set by $H_{{\rm th},\kappa}$, Eq. (9). The scaling properties are $H_{{\rm th},\kappa} \propto d$, $w^{-3/5}$, $j_c^{4/5}$, $n^{-1/5}$, and $\dot{H}_a^{-1/5}$. With typical temperature dependences we have $H_{{\rm th},\kappa} \propto T^{4/5}$ at low T. The w-scaling is consistent with the observed increase of $H_{\rm th}$ with reduced sample width.[20] It is unclear if the $\dot{H}_a$-scaling is consistent with previous experiments since $\dot{H}_a$ is usually not reported in magneto-optical experiments. Yet, that authors of Ref. 32 observed $\dot{H}_a$-dependency of avalanche activity in magnetization measurements and recent experiments showed that high-T_c materials can turn unstable for ramp-rates above 1 kT/s.[15] Third, at deeper penetration the threshold is determined by $H_{{\rm th},h}$, Eq. (12). Close to $T_{\rm th}$ it diverges as

$$H_{{\rm th},h} = \frac{dj_c}{2\pi}\ln\left(\frac{4T_{\rm th}}{T_{\rm th} - T}\right). \qquad (17)$$

The threshold temperature of Eq. (14) scales as $T_{\rm th} \propto T_c^{3/4}$, $d^{1/4}$, $w^{1/4}$, $j_c^{1/4}$, $n_0^{1/4}$, $\dot{H}_a^{1/4}$, and $h_0^{-1/4}$. This result is not obviously in agreement with experimental works, since they usually report a remarkable stable $T_{\rm th}$, such as in MgB_2 where it is close to 10 K.[14] Yet, an indication of $\dot{H}_a$-dependency is that Ref. 33 observed avalanches at 19 K in MgB_2 films under applied current. With regards j_c, the scaling is consistent with Ref. 21, which studied MgB_2 films with anisotropic j_c.

The numerical example of this work used a ramp-rate of 600 mT/s, which is higher than what is used in typical magneto-optical experiments. This means that the predictions of this work should be tested against experiments where the ramp-rate is controlled. Also the cooling parameter, h, should be measured on unstable superconducting films, since the value used in this work is several orders of magnitude smaller than in films with good thermal contact with substrate.[34]

Equation (14) is valid only if $T_{\rm th} \ll T_c$, since the electronic influence on the thermal parameters have been neglected.

VI. CONCLUSIONS

In conclusion, we have derived $H_{{\rm th},\kappa}$, $H_{{\rm th},c}$ and $H_{{\rm th},h}$ based on modes giving rise to undamped oscillations in $\tilde{T}$, $\mathbf{H}$, and $\mathbf{E}$ at the instability threshold. The expressions depend only on measurable material parameters and the experimental control-parameters T and $\dot{H}_a$. The oscillatory modes were found to be much more unstable than the modes considered in previous works, and this may

explain why many material display presence of dendritic flux avalanches, even in magneto-optical imaging experiments, where the external parameters vary slowly.

[1] C. P. Bean, Rev. Mod. Phys. **36**, 31 (1964).
[2] S. L. Wipf, Phys. Rev. **161**, 404 (1967).
[3] P. S. Swartz and C. P. Bean, J. Appl. Phys. **39**, 4991 (1968).
[4] R. G. Mints and A. L. Rakhmanov, Rev. Mod. Phys. **53**, 551 (1981).
[5] S. L. Wipf, Cryogenics **31**, 936 (1991).
[6] A. L. Rakhmanov, D. V. Shantsev, Y. M. Galperin, and T. H. Johansen, Phys. Rev. B **70**, 224502 (2004).
[7] L. Legrand, I. Rosenman, C. Simon, and G. Collin, Physica C **211**, 239 (1993).
[8] R. G. Mints, Phys. Rev. B **53**, 12311 (1996).
[9] M. R. Wertheimer and J. le G. Gilchrist, J. Phys. Chem. Solids **28**, 2509 (1967).
[10] E. Altshuler and T. H. Johansen, Rev. Mod. Phys. **76**, 471 (2004).
[11] P. Leiderer, J. Boneberg, P. Brüll, V. Bujok, and S. Herminghaus, Phys. Rev. Lett. **71**, 2646 (1993).
[12] C. A. Durán, P. L. Gammel, R. E. Miller, and D. J. Bishop, Phys. Rev. B **52**, 75 (1995).
[13] V. Vlasko-Vlasov, U. Welp, V. Metlushko, and G. W. Crabtree, Physica C **341**, 1281 (2000).
[14] T. H. Johansen, M. Baziljevich, D. V. Shantsev, P. E. Goa, Y. M. Galperin, W. N. Kang, H. J. Kim, E. M. Choi, M.-S. Kim, and I. Lee, EPL **59**, 599 (2002).
[15] M. Baziljevich, E. Baruch-El, T. H. Johansen, and Y. Yeshurun, Appl. Phys. Lett. **105**, 012602 (2014).
[16] E. H. Brandt, Phys. Rev. Lett. **76**, 4030 (1996).
[17] I. S. Aranson, A. Gurevich, M. S. Welling, R. J. Wijngaarden, V. K. Vlasko-Vlasov, V. M. Vinokur, and U. Welp, Phys. Rev. Lett. **94**, 037002 (2005).
[18] D. V. Shantsev, A. V. Bobyl, Y. M. Galperin, T. H. Johansen, and S. I. Lee, Phys. Rev. B **72**, 024541 (2005).
[19] D. V. Denisov, A. L. Rakhmanov, D. V. Shantsev, Y. M. Galperin, and T. H. Johansen, Phys. Rev. B **73**, 014512 (2006).
[20] D. V. Denisov, D. V. Shantsev, Y. M. Galperin, E.-M. Choi, H.-S. Lee, S.-I. Lee, A. V. Bobyl, P. E. Goa, A. A. F. Olsen, and T. H. Johansen, Phys. Rev. Lett. **97**, 077002 (2006).
[21] J. Albrecht, A. T. Matveev, J. Strempfer, H.-U. Habermeier, D. V. Shantsev, Y. M. Galperin, and T. H. Johansen, Phys. Rev. Lett. **98**, 117001 (2007).
[22] J. I. Vestgården, D. V. Shantsev, Y. M. Galperin, and T. H. Johansen, Phys. Rev. B **84**, 054537 (2011).
[23] J. I. Vestgården, D. V. Shantsev, Y. M. Galperin, and T. H. Johansen, Sci. Rep. **2**, 886 (2012).
[24] E. H. Brandt, Phys. Rev. B **52**, 15442 (1995).
[25] C. J. Olson, C. Reichhardt, and F. Nori, Phys. Rev. B **56**, 6175 (1997).
[26] E. H. Brandt and M. Indenbom, Phys. Rev. B **48**, 12893 (1993).
[27] R. G. Mints and E. H. Brandt, Phys. Rev. B **54**, 12421 (1996).
[28] J. I. Vestgården, Y. M. Galperin, and T. H. Johansen, J. Low Temp. Phys. **173**, 303 (2013).
[29] The low-T limit of Eq. (12) was considered also in Ref. 27.
[30] J. R. Thompson, K. D. Sorge, C. Cantoni, H. R. Kerchner, D. K. Christen, and M. Paranthaman, Supercond. Sci. Technol. **18**, 970 (2005).
[31] T. H. Johansen, M. Baziljevich, D. V. Shantsev, , P. E. Goa, Y. M. Galperin, W. N. Kang, H. J. Kim, E. M. Choi, and S. I. Lee, Supercond. Sci. Technol. **14**, 726 (2001).
[32] J. Lee, H. Lee, M. Jung, S. Lee, E. Choi, and W. N. Kang, J. Appl. Phys. **107**, 013902 (2010).
[33] A. V. Bobyl, D. V. Shantsev, T. H. Johansen, W. N. Kang, H. J. Kim, E. M. Choi, and S. I. Lee, Appl. Phys. Lett. **80**, 4588 (2002).
[34] E. T. Swartz and R. O. Pohl, Appl. Phys. Lett. **51**, 2200 (1987).